Molecules and Cells

Cariporide Enhances the DNA Damage and Apoptosis in Acid-tolerable Malignant Mesothelioma H-2452 Cells

Yoon-Jin Lee[1,2], Jin-Ho Bae[2], Soo-A Kim[3], Sung-Ho Kim[4], Kee-Min Woo[1], Hae-Seon Nam[2], Moon-Kyun Cho[2], and Sang-Han Lee[1,*]

[1]Department of Biochemistry, College of Medicine, Soonchunhyang University, Cheonan, 31151, Korea, [2]Division of Molecular Cancer Research, Soonchunhyang Medical Research Institute, Soonchunhyang University, Cheonan 31151, Korea, [3]Department of Physical Medicine and Rehabilitation, Cheonan Hospital, Cheonan 31151, Korea, [4]Department of Chemistry, College of Natural Sciences, Soonchunhyang University, Asan 31538, Korea
*Correspondence: m1037624@sch.ac.kr
http://dx.doi.org/10.14348/molcells.2017.0059
www.molcells.org

The Na^+/H^+ exchanger is responsible for maintaining the acidic tumor microenvironment through its promotion of the reabsorption of extracellular Na^+ and the extrusion of intracellular H^+. The resultant increase in the extracellular acidity contributes to the chemoresistance of malignant tumors. In this study, the chemosensitizing effects of cariporide, a potent Na^+/H^+-exchange inhibitor, were evaluated in human malignant mesothelioma H-2452 cells preadapted with lactic acid. A higher basal level of phosphorylated (p)-AKT protein was found in the acid-tolerable H-2452AcT cells compared with their parental acid-sensitive H-2452 cells. When introduced in H-2452AcT cells with a concentration that shows only a slight toxicity in H-2452 cells, cariporide exhibited growth-suppressive and apoptosis-promoting activities, as demonstrated by an increase in the cells with pyknotic and fragmented nuclei, annexin V-PE(+) staining, a sub-G_0/G_1 peak, and a G_2/M phase-transition delay in the cell cycle. Preceding these changes, a cariporide-induced p-AKT down-regulation, a p53 up-regulation, an ROS accumulation, and the depolarization of the mitochondrial-membrane potential were observed. A pretreatment with the phosphatidylinositol-3-kinase (PI3K) inhibitor LY294002 markedly augmented the DNA damage caused by the cariporide, as indicated by a much greater extent of comet tails and a tail moment with increased levels of the p-histone H2A.X, p-ATM^{Ser1981}, p-ATR^{Ser428}, p-CHK1^{Ser345}, and p-CHK2^{Thr68}, as well as a series of pro-apoptotic events. The data suggest that an inhibition of the PI3K/AKT signaling is necessary to enhance the cytotoxicity toward the acid-tolerable H-2452AcT cells, and it underlines the significance of proton-pump targeting as a potential therapeutic strategy to overcome the acidic-microenvironment-associated chemotherapeutic resistance.

Keywords: cariporide, LY294002, malignant mesothelioma, p53, phosphatidylinositol-3-kinase

INTRODUCTION

Malignant mesothelioma (MM) is a rare but aggressive tumor, and its incidence appears to be rising over the past two decades due to the increase in asbestos-exposure cases. The median overall survival for patients is 1.05 years, and the poor prognosis is attributed to a high resistance to chemotherapeutic agents and the delayed diagnosis that is due to a long latency period, and (Skammeritz et al., 2011). Despite the development of various therapeutic strategies, the emergence of drug-resistant variants as the disease progresses

Received 17 April, 2017; revised 3 July, 2017; accepted 9 July, 2017; published online 10 August, 2017

eISSN: 0219-1032

currently appears inevitable.

The tumor microenvironment is often hypoxic owing to the reduced perfusion in which the preferential alteration of the energy metabolism into a high rate of glycolysis produces a large quantity of lactate as the glucose breakdown product, and this even occurs with an abundant-oxygen exposure (Warburg, 1956). The subsequent efflux of the H^+ outside cancer cells, mediated by the function of proton transporters or pumps, and the resultant decrease in the extracellular pH (pHe) within the tumor microenvironment play critical roles in the driving of the malignant progression including the cell migration and the resistance to various chemotherapeutic agents (De Milito and Fais, 2005). The hostile conditions within the tumor microenvironment, such as the acidic pHe, hypoxia, and nutrient deprivation, help cancer cells induce a concerted rapid change in their gene-expression pattern, and they activate several signaling pathways for the purpose of survival (Rohwer and Cramer, 2011). The metabolic reprogramming contributes to the selection of the cells that are capable of adapting to various stress conditions, and that eventually lead to a cellular state that exhibits an enhanced resistance to these conditions (Alfarouk, 2016; Yoshida, 2015).

The phosphatidylinositol-3-kinase (PI3K)/AKT survival pathway is one of the major signaling cascades, and is related to the acquisition of chemoresistance in various types of human cancers including MM (Guerrero-Zotano et al., 2016; Ramos-Nino and Littenberg, 2008; Wilson et al., 2015). The activation of the PI3K can phosphorylate its downstream targets, including the AKT, and subsequently activate various molecules that are involved in protein synthesis and cell growth. In prostate cancer and esophageal adenocarcinoma cells, exposure to an acidic pH induces the AKT activation, which is correlated with an enhanced cell survival (Lee et al., 2013; Souza et al., 2002). The phosphorylated AKT also inhibits p53 activation by enhancing the MDM2 (mouse double minute 2 homolog)-mediated ubiquitination for a proteasomal degradation, consequently inhibiting the mitochondrial p53-dependent apoptosis (Fenouille et al., 2011). Therefore, the clinical implications of the inhibition of the PI3K/AKT pathway are important for the suppression of the emergence of a chemotolerant phenotype and the switching of the cell-survival signaling to death.

The Na^+/H^+-exchanger isoform-1 (NHE1) is responsible for the maintenance of the intracellular pH (pHi) homeostasis within tumor cells (acidic pHe of 6.8 vs. alkaline pHi of 7.4), for which it promotes the reabsorption of extracellular Na^+ and the extrusion of intracellular H^+ (Lee et al., 2015). Earlier studies have shown that a long-term incubation in low-pH media or metabolic acidosis enhances the expression and function of NHE1 (Casey et al., 2010; Igarashi et al., 1992). It has been shown that both acidic pHe and NHE1 activity increase the invasive capability of tumor cells and are engaged in the resistance to various anticancer drugs (Ma et al., 2015, Rofstad et al., 2006).

Research has shown that cariporide, a selective inhibitor of NHE1, is non-toxic in mammalian cells (Wong et al., 2002); therefore, this agent might be used to sensitize acidic pHe-tolerant cells to some chemotherapeutic agents through its causing of a low pHi through the disruption of the intra-extracellular pH gradient.

In the present study, the anticancer effects and potential mechanisms of cariporide were evaluated, and the involvement of the PI3K/AKT pathway was characterized in the acid-tolerable MM H-2452AcT cells using its specific inhibitor LY294002.

MATERIALS AND METHODS

Reagents and cell culture

Cariporide, LY294002, 3-(4,5-dimethylthiazol-2-yl)-2,5-diphenyltetrazolium bromide (MTT), Rhodamine 123, propidium iodide (PI), DAPI, 2',7'-dichlorodihydrofluorescein diacetate (DCF-DA), and the β-actin antibody (A2228) were obtained from Sigma-Aldrich (Merck KGaA, Germany). The antibodies against B-cell lymphoma 2 (2820; Bcl-2), cyclin B1 (12231), phosphorylated (p)-cyclin dependent kinase 2 (9114; p-Cdc2^{Thr161}), AKT (9272), p-AKT (9271), PARP (9542), procaspase-3 (9665), cleaved caspase-3 (9664), p-histone H2A.X (9718), p-ATM (5883), p-ATR (2853), p-CHK1 (2348), and p-CHK2 (2197) were purchased from Cell Signaling Technology, Inc. (USA). The antibodies against p53 (sc-126), goat anti-rabbit IgG-HRP (sc-2004), goat anti-mouse IgG-HRP (sc-2005), and the Enhanced Chemiluminescence (ECL) kit were purchased from Santa Cruz Biotechnology, Inc. (USA). The human malignant-mesothelioma cell line H-2452 was obtained from the American Type Culture Collection (ATCC; USA). The H-2452 cells were maintained at 37℃ in an RPMI-1640 medium (SH30027.01; GE Healthcare Life Sci., Australia) supplemented with 10% fetal bovine serum (SH30084.03; GE Healthcare Life Sci.), 100 U/ml penicillin, and 100 μg/ml streptomycin. The acidic pH-tolerable H-2452 cells (H-2452AcT) were generated from parental-control H-2452 cells (H-2452) through the application of a continued exposure to 3.8 μM lactic acid. The cells were serially passaged four times for 12 days in a culture medium containing lactic acid, after which time the cells were grown to a 70% confluence in a submerged monolayer culture for 24 h prior to the treatment.

MTT assay

The cell viability was measured using the MTT assay. The cells (5×10^3 cells/well) were seeded onto 96-well microtiter plates and incubated with the vehicle [0.1% dimethylsulfoxide (DMSO) in medium], cariporide (0 μM, 40 μM, 80 μM, 160 μM, 240 μM, and 320 μM), LY294002 (0 μM, 2.5 μM, 5 μM, 7.5 μM, 10 μM, and 20 μM), or pretreated with LY294002 (5 μM) for 2 h prior to cariporide (160 μM) treatment for 48 h and 72 h at 37°C, and were then exposed to tetrazolium dye (final concentration = 0.1 mg/ml) for 4 h at 37°C. The absorbance value at the 540 nm wavelength was measured using the GloMax-Multi Microplate Multimode Reader (Promega Corporation, USA). The percentage of viable cells was determined by comparing the results with those of the vehicle-treated control cells (100%).

Western blot analysis

The cells (10^5 cells/well) were seeded onto a six-well culture

plate and were then pretreated with the LY294002 (5 μM) or vehicle for 2 h prior to the cariporide (160 μM) for the indicated times. The cells were lysed in an RIPA buffer [1 x phosphate buffered saline (PBS), 1% NP-40, 0.5% sodium deoxycholate, 0.1% SDS, 10 μg/ml phenylmethanesulfonyl fluoride, and a protease-inhibitor cocktail tablet (Boehringer Mannheim, Germany)] for 30 min on ice, and then they were pelleted by a centrifugation of 10,000 g for 10 min at 4℃. The protein concentration was determined using the Pierce™ BCA Protein Assay kit (23225, Thermo Scientific, USA), according to the manufacturer's protocol. The cell lysates containing 40 μg of protein were separated on the NuPAGE 4% to 12% Bis-Tris polyacrylamide gels (Invitrogen; Thermo Fisher Scientific, Inc., USA), and they were subsequently electrophoretically transferred to western-blot polyvinylidene fluoride membranes (Bio-Rad Laboratories, Inc., USA). The membrane was incubated overnight at 4℃ with a ratio of 1:500 diluted primary antibodies in the case of the blocking buffer (B6429; Sigma-Aldrich, Germany), followed by a 2 h incubation at room temperature with a 1:5,000 dilution rate of the secondary antibody coupled to the horseradish peroxidase. Immunoreactive bands were visualized using an ECL detection kit and X-ray film. The blots were stripped using a stripping buffer (100 mM β-mercaptoethanol, 2% SDS, and 62.5 mM Tris-HCl, pH 6.7) and re-probed with an anti-β-actin antibody that served as the loading control.

RNA interference assay

An RNA interference assay was performed using a p53-targeting siRNA duplex (HSS186390; Invitrogen). Briefly, the cells were seeded onto six-well and 96-well plates and then transfected at a 40% confluency with a p53-targeting siRNA duplex, or the Stealth RNAi negative-control duplex (12935-200; Invitrogen) using lipofectamine RNAi MAX (Invitrogen) according to the manufacturer's recommendations, after which time they were processed for the MTT assay and the western blotting.

DAPI staining

Nuclear morphology was observed with the use of DAPI (4',6-diamidino-2-phenylindole) staining. The cells (1×10^5 cells/well) were seeded onto the cover slip in the six-well culture plate and then pretreated with the LY294002 (5 μM) or vehicle for 2 h prior to the cariporide (160 μM) for 72 h at 37℃. The cover slip for adherence cells were washed with 1x PBS 3 times, fixed in 4% paraformaldehyde at room temperature for 10 min, and washed with 1x PBS. The cover slip was resuspended in the DAPI (3 ng/ml in 1x PBS) for 5 min in the dark and washed with 1x PBS. The cover slip was placed on the slides, and was then mounted using a mounting medium (08381; Polysciences, Inc., USA). The apoptotic cells were observed with the FluoView FV10i confocal fluorescence microscope (Olympus Corporation, Japan).

Annexin V-PE binding assay

The apoptotic-cell distribution was determined using the Muse Annexin V & Dead Cell Assay kit (MCH100105; Merck KGaA, Germany) according to the manufacturer's protocol. The kit includes a fluorescent-dye phycoerythrin (PE) that is conjugated to the annexin V to detect the phosphatidylserine on the external membrane of the apoptotic cells and the 7AAD (7-amino-actinomycin D) as a dead-cell marker. Briefly, the cells (1×10^5 cells/well) were seeded into the six-well culture plate and pretreated with the LY294002 (8 μM) or vehicle for 2 h prior to the cariporide (160 μM) for 72 h at 37℃. The cells were trypsinized and collected into a culture medium, mixed with the Muse™ Annexin V & Dead Cell reagent, and analyzed using the Muse Cell Analyzer (Merck KgaA, Germany).

Cell cycle analysis

The percentages of the cells in the G_1, S, and G_2/M phases were measured according to the quantitation of the DNA content in the PI-stained cells. The cells (1×10^5 cells/well) were seeded onto the six-well plates and pretreated with the LY294002 (5 μM) or vehicle for 2 h prior to the cariporide (160 μM) for 72 h at 37℃. The trypsinized cells (~10^6 cell/ml) were pelleted by centrifugation at 500 g for 7 min at 4℃, fixed in 70% ice-cold ethanol overnight at -20℃, and incubated with the Muse™ Cell Cycle reagent (Merck Millipore, USA). The data from 10,000 single-cell events were collected using the MACSQuant Analyzer and analyzed using the MACSQuantify™ v2.5 software (MiltenyiBiotec GmbH, Germany).

Alkaline comet assay

The single cell gel electrophoresis was performed using the Comet Assay kit (4250-050-K; Trevigen, USA) according to the manufacturer's protocol. Briefly, the cells (1×10^5/ml) were mixed with molten LM (low melting point) agarose at a ratio of 1:10 (v/v) and layered onto the CometSlide™. The slides were then incubated with the lysis solution at 4℃ for 45 min and the Alkaline Unwinding solution for another 20 min at room temperature. Following an electrophoresis at 21 V for 30 min, the slides were washed with dH_2O for 5 min and treated with the 70% ethanol for 5 min. The dried slides were stained with SYBR green (4309155; Thermo Fisher Scientific, Inc., USA) at 4℃ for 5 min in the dark and were observed with the FluoView FV10i confocal fluorescence microscope. Ten images were randomly captured per slide, and the tail-moment values of 60 cells were scored per slide using the fluorescence microscope with the Comet Assay IV v4.3 software (Perceptive Instruments Ltd., UK).

Measurement of intracellular ROS levels

The intracellular ROS (reactive oxygen species) levels were evaluated by measuring the DCF-DA (Sigma-Aldrich, Germany) fluorescence intensity. The cells (1×10^5 cells/well) were seeded onto the six-well culture plate and pretreated with the LY294002 (5 μM) or vehicle for 2 h prior to the cariporide (160 μM) for 72 h at 37℃. The cells were trypsinized, pelleted by centrifugation at 500 g for 7 min at 4℃, and resuspended in a serum-free RPMI-1640 medium containing 10 μM DCF-DA for 30 min at 37℃ in the dark. Following the incubation, the cells were trypsinized, resuspended in 1× PBS, and immediately analyzed with the MACSQuant Analyzer and MACSQuantify™ v2.5 software (Miltenyi Biotec GmbH, Germany). The DCF (2',7'-dichlorofluorescein) fluores-

cence was detected using a 530 nm bandpass filter.

Mitochondrial membrane potential (ΔΨm) analysis

The cells (1×10^5 cells/well) were seeded onto the six-well plates and pretreated with the LY294002 (5 μM) or vehicle for 2 h prior to the cariporide (160 μM) for 72 h at 37℃. The cells were trypsinized, harvested by centrifugation at 500 g for 7 min at 4℃, washed twice with the PBS, and stained with a serum-free RPMI-1640 medium containing Rhodamine 123 (final concentration = 30 nM) at 37℃ for 30 min. Following the incubation, the cells were washed twice with 1x PBS. The fluorescence intensity was measured and analyzed using the MACSQuant analyzer and the MACSQuantify™ v2.5 software (Miltenyi Biotec GmbH, Germany), respectively.

Statistical analysis

The statistical comparisons were performed using a one-way analysis of variance, followed by Tukey's post-hoc correction for multiple comparisons, and the SPSS v17.0 was used (SPSS, Inc., USA). Data are expressed as the mean ± standard deviation for three independent experiments. A $P < .05$ was considered statistically significant compared to the respective H-2452 controls.

RESULTS

Long-term incubation of H-2452 cells under low pH media shows a high level of AKT phosphorylation

A prolonged incubation of H-2452 cells under an acidic medium was employed to induce an acidic tolerance. Acidic pHe-tolerable H-2452AcT cells were generated from their parental H-2452 cells using a serial passaging that was conducted four times for 12 days in a culture medium containing 3.8 μM lactic acid, after which time the MTT assay was used to measure the cell viability. As expected, the H-2452AcT cells are more tolerant to low-pH media together with an enhanced-percent cell viability compared with the H-2452 cells (Fig. 1A). In addition, the activation of PI3K, as demonstrated by the increased phosphorylation of the AKT level, was more increased in the H-2452AcT cells in a time-dependent experiment. Switching to a fresh-culture media without lactic acid expressed a slower-growth phenotype in the H-2452AcT cells; however, the level of p-AKT remained increased compared with the H-2452 cells (Fig. 1B), although an obvious change in the cell cycle distribution was not found between the two cell lines (Fig. 1C).

Cariporide and LY294002 inhibit the AKT phosphorylation and up-regulate the p53 expression level in the H-2452AcT cells

The cariporide treatment significantly inhibited the growth of the H-2452AcT cells at a concentration that shows no significant toxicity in the H-2452 cells, whereas a PI3K inhibitor, LY294002, showed the equivalent cytotoxicity level on both cell lines (Figs. 2A and 2B). However, the combined cariporide (160 μM)/LY294002 (5 μM) treatment for 48 h showed a more potent cytotoxicity in the H-2452AcT cells

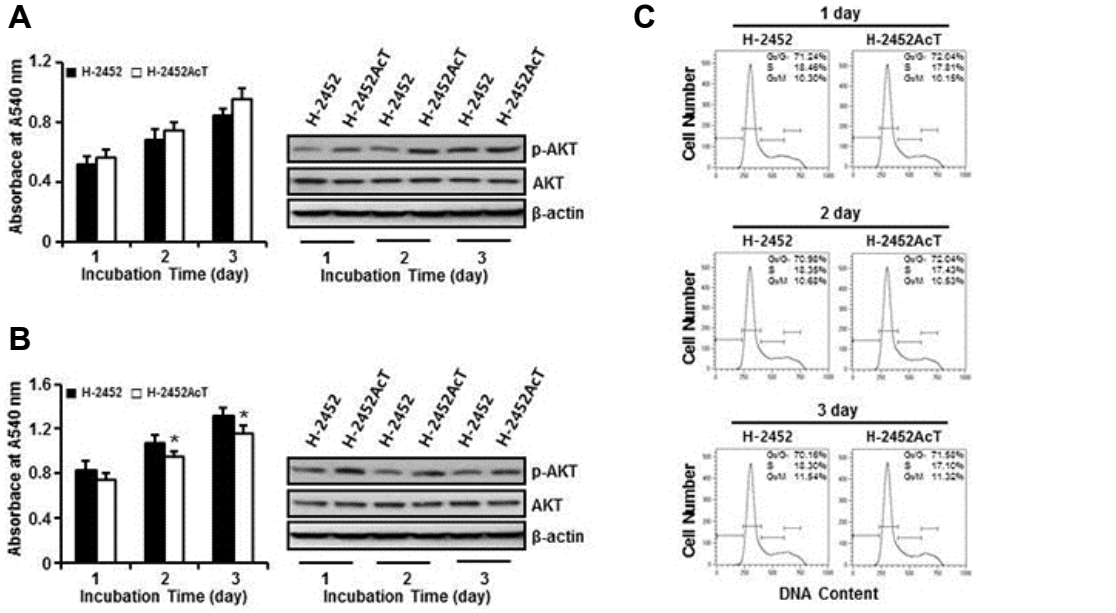

Fig. 1. Cell growth and phosphorylation status of AKT in acid-tolerable H-2452AcT cells. (A, B) H-2452 and H-2452AcT cells were incubated with the RPMI-1640 medium containing (a) or not containing (b) 3.8 μM of lactic acid for 24 h, 48 h, and 72 h. The cell viability and p-AKT level were determined using an MTT assay and a western-blot analysis, respectively. (C) Cells were incubated with the RPMI-1640 medium without lactic acid for 24 h, 48 h, and 72 h. The cell distributions in the sub-G_0/G_1, G_0/G_1, S, and G_2/M phases were analyzed using flow cytometry following a propidium-iodide staining (20 μg/ml). The error bars indicate the mean ± standard deviation for three independent experiments. The β-actin was used as a loading control. $^*P < .05$ vs. the respective H-2452 controls.

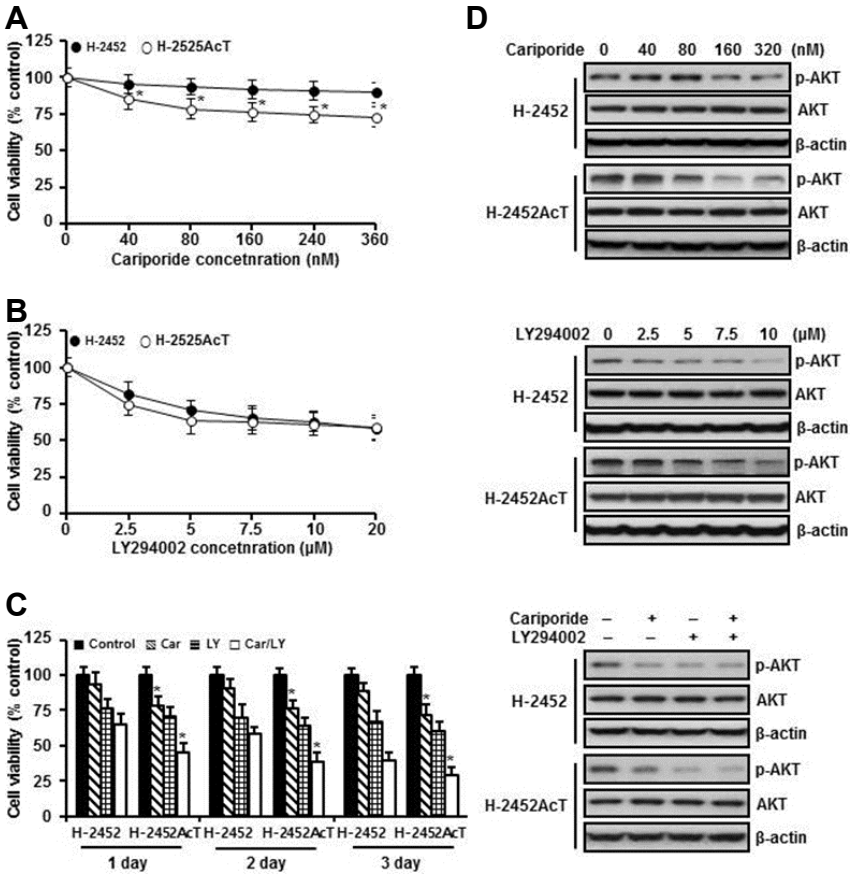

Fig. 2. Effects of cariporide and LY294002 on the cell growth and phosphorylation status of AKT in H-2452 and H-2452AcT cells. (A, B) The cells were incubated with the vehicle (0.1% DMSO) or various concentrations of cariporide (40 μM to 360 μM) alone (a) or LY294002 (2.5 μM to 20 μM) alone (b) for 48 h. (C) Cells were treated with cariporide (160 μM) and LY294002 (5 μM), alone or in combination, for 24 h, 48 h and 72 h. The cell viability was determined using an MTT assay. The p-AKT levels were determined by the western-blot analysis. The error bars indicate the mean ± standard deviation for three independent experiments. The β-actin was used as a loading control. $^{*}P < .05$ vs. the respective H-2452 controls. Car, cariporide; LY, LY294002; Car/LY, the combination treatment of cariporide and LY294002.

compared with their parental H-2452 cells, leading to a significant decrease in the cell viability (38.7% and 57.9%, respectively) compared with each of the cariporide (76.9% and 91.1%, respectively) or LY294002 (64.4% and 70.5%, respectively) treatments alone (Fig. 2C).

The underlying mechanism of the chemosensitizing effects of the cariporide to the LY294002 was then further investigated. Treatment with cariporide and LY294002, alone or in combination, led to an apparent decrease in the p-AKT levels of both cell lines (Fig. 2D). With the increasing concentration, an increase in the levels of the p53 protein was also detected by the treatment with the cariporide or the LY294002 alone in the H-2452AcT cells, separate from the H-2452 cells (Fig. 3A). The cariporide/LY294002 combination treatment induced an increase in the p53/Bcl-2 protein ratio and the cleaved form of the caspase-3, along with a decreased level of its substrate PARP, in the H-2452AcT cells; however, these changes are much greater in the H-2452AcT cells compared with the H-2452 cells (Fig. 3B). To evaluate a possible role of the endogenous p53 on cell growth, the cells were transfected with p53-targeting siRNAs and their sensitivity to the cell viability was investigated. As expected, a knockdown of the p53 increased the growth of both the H-2452 and H-2452AcT cells in a time-course experiment (Fig. 3C). Overall, the findings of the current study indicate that, together with an increased p53/Bcl-2-protein ratio, the suppression of the AKT phosphorylation following the treatment with the cariporide and the LY294002 may play a crucial role in the inducement of a marked cytotoxicity in H-2452AcT cells.

Cariporide and LY294002 promote apoptosis and increase the DNA damage in H-2452AcT cells

To further investigate whether the cariporide/LY294002-based growth inhibition of the H-2452AcT cells is related to apoptotic cell death, the pro-apoptotic effects of the two compounds were examined by analyzing the nuclear phenotypes and the apoptotic cells using DAPI and annexin-V-phycoerythrin (PE) staining, respectively. The proportion of the adherent cells with the condensed and fragmented nuclei is much higher than that of the H-2452 cells (Fig. 4A), and the proportion of the annexin-V-PE(+) cells that underwent the apoptosis in the early and late phases increased to 67.98% in the H-2452AcT cells treated with the cariporide and the LY294002 in combination compared with the H-2452 cells (48.37%) (Fig. 4B). Additionally, the cell cycle analysis indicated an increase in the sub-G_0/G_1 peak, a hallmark of apoptosis, and an increase of the cell percentage at the G_2/M phase with a decrease of the cells at the G_1 and S phases indicated a G_2-to-M phase transition delay (Fig. 5A). The levels of the cell cycle regulatory proteins for the G_2-to-M-phase transition such as cyclin B1 and p-cdc2 (Thr^{161}) were also down-regulated following the treatment with the

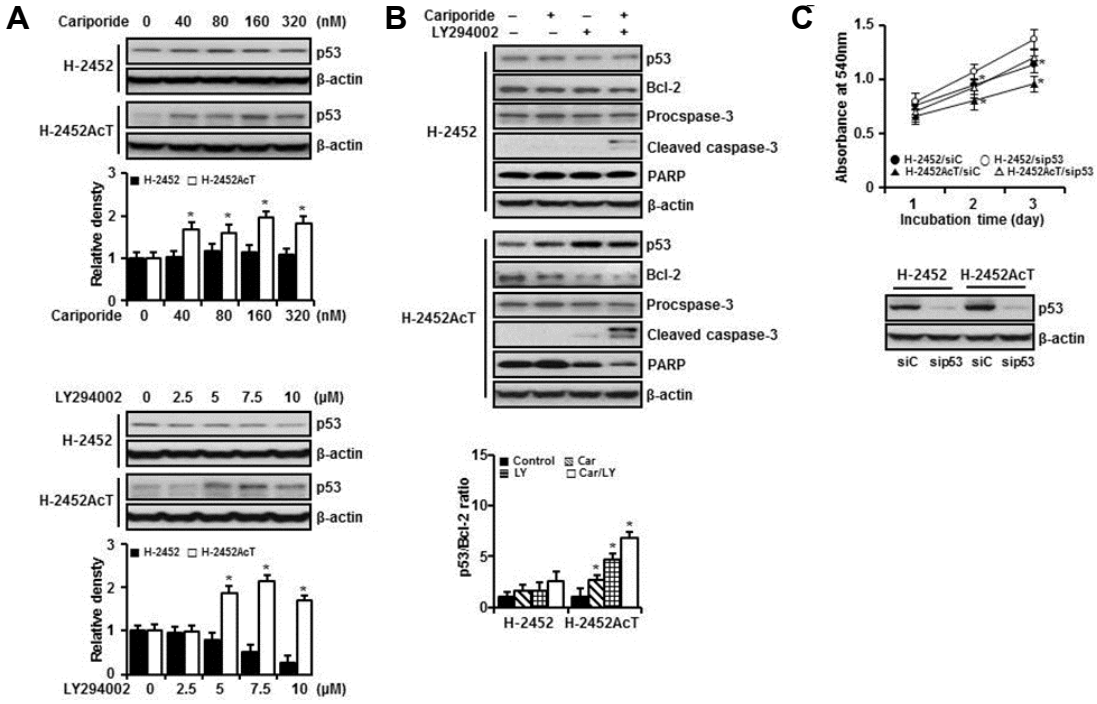

Fig. 3. Effects of cariporide and LY294002 on the levels of p53 and apoptosis-regulating proteins in H-2452 and H-2452AcT cells. (A, B) The cells were incubated with the vehicle (0.1% DMSO) or various concentrations of cariporide (40 μM to 320 μM) and LY294002 (2.5 μM to 10 μM), alone (a) or in combination (160 μM cariporide and 5 μM LY294002) (b) for 48 h. The protein levels were determined by the Western-blot analysis. The p53/Bcl-2 expression ratio and relative density of protein bands were obtained from densitometric analysis of the Western blot images normalized to β-actin. Representative results are presented from one of three independent experiments; β-actin was used as a loading control. (C) The cells were transfected with 10 nM p53-targeting siRNA (sip53) or Stealth RNAi control siRNA (siC) for 24 h, 48 h and 72 h. The cell viability and p-AKT level were determined using an MTT assay and a Western-blot analysis, respectively. The error bars indicate the mean ± standard deviation for three independent experiments. The β-actin was used as a loading control. $^{*}P < .05$ vs. the respective H-2452 controls. Bcl-2, B-cell lymphoma 2; PARP, poly (ADP-ribose) polymerase. Car, cariporide; LY, LY294002; Car/LY, the combination treatment of cariporide and LY294002.

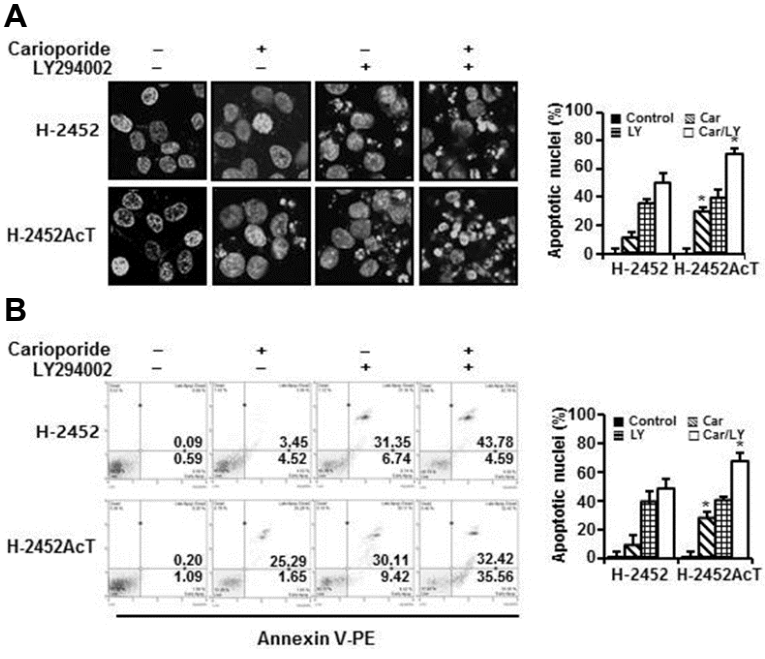

Fig. 4. Apoptosis-promoting effects of cariporide and LY294002 in H-2452 and H-2452AcT cells. The cells were treated with cariporide (160 μM) and LY294002 (5 μM), alone or in combination, for 72 h. (A) Nuclear morphology was assessed by nuclear staining with DAPI (magnification ×40). (B) The number of apoptotic cells following annexin V-PE staining was analyzed using a Muse Cell Analyzer. Representative results are presented from one of three independent experiments. Error bars indicate the mean ± standard deviation for three independent experiments. $^{*}P < .05$ vs. the respective H-2452 controls. Car, cariporide; LY, LY294002; Car/LY, the combination treatment of cariporide and LY294002; PE, phycoerythrin.

cariporide and the LY294002 in both the H-2452AcT and H-2452 cells (Fig. 5B).

To assess the effects of the cariporide and the LY294002 on the DNA damage in the H-2452AcT cells, the comet assay (single cell gel electrophoresis) was employed under non-denaturing conditions. As shown in Fig. 5C, the cariporide and the LY294002, alone or in combination, showed a significant increase of the damaged DNA fragments, which was represented by a much greater extent of comet tails and the tail moment compared with the untreated controls. The tail-moment value increased to 53.08% in the H-2452AcT cells treated with the two compounds compared with the H-2452 cells (43.22%). Next, the phosphorylation status of the various damage-sensing molecules such as ATM/ATR, CHK1/2, and histone H2AX were examined following the treatment with the cariporide and the LY294002, alone or in combination. As shown in Fig. 5D, the levels of p-ATM^{Ser1981} and p-ATR^{Ser428}, as well as their respective downstream targets p-CHK1^{Ser345} and p-CHK2^{Thr68} were increased in both of the cell types, which were accompanied by an increase of the phospho-H2A.X^{Ser139} (γ-H2A.X), a known marker of the DNA double-strand breaks (DSBs).

Cariporide and LY294002 cause ROS accumulation and mitochondrial dysfunction

To investigate whether the cytotoxic effects of the cariporide and the LY294002 on the H-2452AcT cells are associated with oxidative mitochondrial damage, the intracellular-ROS levels and the mitochondrial membrane potential (ΔΨm) were measured using flow cytometry with the ROS-sensitive fluorophore DCF-DA and the Rhodamine 123, respectively. As shown in the representative histogram in Fig. 6A, the treatment with each of the cariporide or the LY294002 alone increased the ROS level in the H-2452AcT cells (27.68% or 40.90%, respectively) or the H-2452 cells (9.62% or 39.78%, respectively) compared with their respective controls, as indicated by the DCF-fluorescence shift to the right. The cariporide/LY294002 combination treatment the increased the ROS level to approximately 66.45% and 47.46% in the H-2452AcT and H-2452 cells, respectively. Similarly, the proportion of cells with the ΔΨm loss, as indicated by the Rhodamine-123-fluorescence shift to the left, significantly increased to 26.86% or 67.05% in the H-2452AcT cells treated with the cariporide alone or in combination with the LY294002, respectively, compared with the H-2452 cells (9.37% or 37.12%, respectively).

DISCUSSION

The acidic pHe is the well-known feature of the tumor microenvironment, and it may play a pivotal role in the emergence of cells with an increased resistance to many

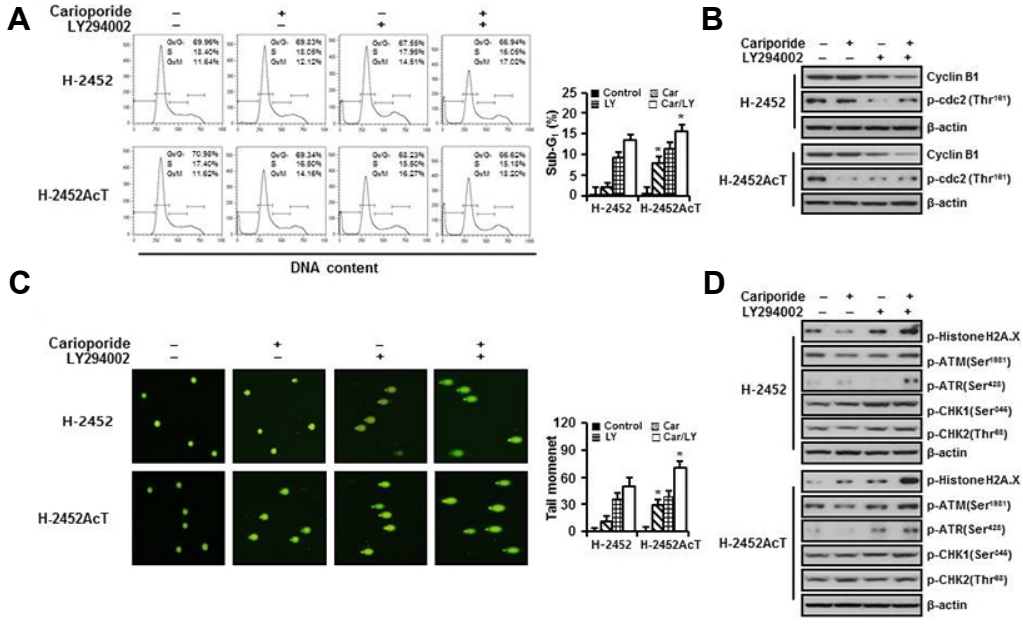

Fig. 5. Effects of cariporide and LY294002 on the cell cycle and DNA damage in H-2452 and H-2452AcT cells. The cells were treated with cariporide (160 μM) and LY294002 (5 μM), alone or in combination, for 72 h. (A) The cell distributions in the sub-G_0/G_1, G_0/G_1, S, and G_2/M phases were analyzed using flow cytometry following a propidium-iodide staining (20 μg/ml). (B) Expression levels of cell cycle-regulating molecules were measured by Western blot analysis. (C) The alkaline comet assay was conducted to assess DNA damage. The tail moment were scored per slide using the fluorescence microscope with the Comet Assay IV v4.3 software. (magnification ×40). (D) Expression levels of DNA damage-sensing molecules were measured by Western blot analysis. The β-actin was used as a loading control. Error bars indicate the mean ± standard deviation for three independent experiments. $^{*}P < .05$ vs. the respective H-2452 controls. Car, cariporide; LY, LY294002; Car/LY, the combination treatment of cariporide and LY294002; p-cdc2, phosphorylated cyclin dependent kinase 2.

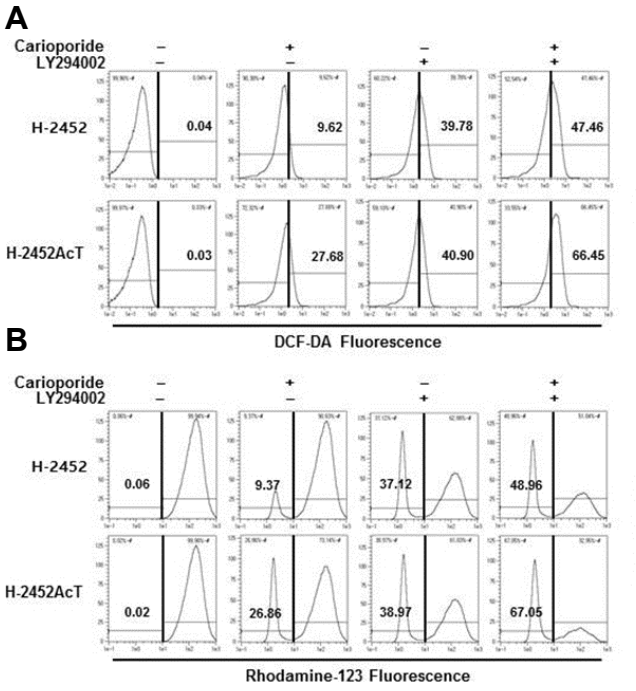

Fig. 6. Effects of cariporide and LY294002 on ROS generation and mitochondrial membrane potential (ΔΨm) in H-2452 and H-2452AcT cells. The cells were treated with cariporide (160 μM) and LY294002 (5 μM), alone or in combination, for 72 h. (A) The levels of cellular ROS were measured using flow cytometry following staining with DCF-DA (10 μM). A shift in DCF fluorescence to the right indicated an increase in ROS (reactive oxygen species) levels. (B) ΔΨm was measured by staining the cells with Rhodamine 123 (30 nM). The error bars indicate the mean ± standard deviation for the three independent experiments. $^{*}P < .05$ vs. the respective H-2452 controls. DCF-DA, 2',7'-dichlorodihydrofluorescein diacetate; Car, cariporide; LY, LY294002; Car/LY, the combination treatment of cariporide and LY294002.

chemotherapeutic agents (Raghunand and Gillies, 2000). Such an unfavorable intra-tumor environment may activate several different mechanisms that alter the phenotype of the tumor cells; of these, the PI3K/AKT survival pathway is frequently activated at different levels in many types of cancers and plays critical roles in the promotion of the growth, proliferation, and survival of the cancer cells (Ramos-Nino and Littenberg, 2008; Wilson et al., 2015). The aim of the present study comprises the anticancer effects and potential mechanisms of an NHE1 inhibitor cariporide and a PI3K inhibitor LY294002 on acidic pHe-tolerable MM H-2452AcT cells, as demonstrated by the enhancement of the apoptosis and the G_2/M phase transition delay in the cell cycle. These findings at least partly provide a mechanistic explanation that is related to the increased DNA damage to the H-2452AcT cytotoxicity that is caused by the two compounds.

The activation of the PI3K is reportedly induced after the acid loading, possibly as an adaptive pro-survival process, in various cancer types including the prostate cancer and lung cancer cells *in vitro* (Hu et al., 2016; Lee et al., 2013). To date, there is little information to indicate how acidic pHe affects activation of PI3K/AKT signaling at the molecular level. It is known that ion transporters, such as NHE1, are activated by acid exposure (low pHe) to export excess H^+ ions from the cytoplasm to the extracellular environment, which subsequently leads to the activation of the PI3K/AKT signaling by an ezrin/radixin/moesin-dependent mechanism (Wu et al., 2004). In addition to its antiapoptotic role, AKT has been shown to play a role in the prevention of cytosolic acidification (Gottlob et al., 2001). Consistent with the previous studies, the prolonged exposure of the H-2452 cells to lactic acid exhibited an increased AKT phosphorylation, which remained increased even when the lactic acid was replaced with a fresh-culture media without lactic acid, compared with their parental H-2452 cells. This indicates that the activation of the PI3K may affect the increased tolerance of the H-2452AcT cells to acidic environments. Therefore, it can be rational to speculate that intracellular acidification by NHE1 inhibitors may inhibit AKT activation and be useful in inhibiting the proliferation of cells that are situated in slightly acidic tumor microenvironment. This notion is supported by the findings that amiloride, another NHE1 inhibitor, inhibits AKT phosphorylation in many cell types (Kim and Lee, 2005; Zheng et al., 2015) and by our demonstration that cariporide provides a signal that antagonizes AKT activation.

The inhibition of the PI3K activity and the subsequent inactivation of its downstream substrate, AKT, sensitize various cancer cells to cisplatin and doxorubicin (Fan et al., 2014; Singh et al., 2013). At the concentrations that exhibited a slight cytotoxicity on the H-2452 cells, the cariporide treatment inhibited the AKT phosphorylation in both the H-2452AcT and H-2452 cells. A further inhibition of the PI3K activity in combination with the LY294002 caused a marked cytotoxicity in the H-2452AcT, as demonstrated by a series of mitochondrial pro-apoptotic events, including an increased p53/Bcl-2 expression ratio, a marked ΔΨm loss, and the subsequent activation of the executioner caspase-3 along with the DNA damage and the cell cycle transition delay from the G_2 phase to the M phase. These cellular responses are associated with the effects of the two compounds on the p53 expression. Wild-type p53 is required for the sensitization of chemoresistant cancer cells via the inhibition of the PI3K pathway components. It has been reported that p53 binds to the PIK3CA promoter to suppress the transcription of the p110α catalytic subunit of PI3K, which even-

tually inhibits the phosphorylation of its target substrate, AKT, by reducing the protein level and the activity of the PI3K in ovarian-cancer cells (Astanehe et al., 2008). AKT can also inversely inhibit the p53 activation through the MDM2 and therefore inhibits the mitochondrial p53-dependent apoptosis (Fenouille et al., 2011). Similarly, the inhibition of the AKT phosphorylation from the combination treatment of the cariporide and the LY294002 in the present study increased the p53-protein level along with an increased cytotoxicity, while a p53 knockdown resulted in enhanced cell viability. These results indicate that p53 may exert suppressive effects on the cell growth through the PI3K/AKT signaling. How a decrease in the pHi affects the p53 expression is not known. However, as noted above, cross-talk between AKT activity and p53 expression should be considered. The tumor-suppressing p53 protein drives the gene expression for DNA repair, growth arrest, and apoptosis (Pabla et al., 2008; Polager and Ginsberg, 2009). When DNA is damaged before the DNA synthesis or mitosis, the cells with remediable damage stop their cell cycle progression at the G_1 or G_2 phase until the damage is repaired; however, irreversibly damaged cells are eliminated by apoptosis. It has been demonstrated that the inactivation of the p53 protein is associated with an increase of the Bcl-2 anti-apoptotic protein, which has been responsible for anticancer-drug resistance in various cancers (Schmitt and Lowe, 2001; Weller, 1998). In this regard, the presence of an upregulated p53 expression, a downregulated Bcl-2 expression, and an inhibited pro-survival PI3K/AKT signaling, which suppresses the actions of the pro-apoptotic circuitry, may provide a theoretical basis for the production of an apoptosis-promoting effect through the application of cariporide and LY294002 in H-2452AcT cells.

Not only does p53 exert a strong influence on apoptosis, but it also plays a central role in the DNA-damage triggered responses, as outlined above. The findings of this study show that the treatment with cariporide and LY294002 cause a marked increase in the level of the γ-H2A.X, a commonly assayed marker of DSBs, thereby indicating that a series of pro-apoptotic processes might be the result of DSB-related DNA damage (Tomita, 2010). DNA damage induces the subsequent activation of DNA-repair proteins as well as DNA-damage checkpoints to arrest the cell cycle, whereby the repair-process time is allowed for (Deng et al., 2015). Accordingly, the key regulators of the DNA-damage response such as p-ATM^{Ser1981} and p-ATR^{Ser428}, as well as their respective downstream targets p-CHK1^{Ser345} and p-CHK2^{Thr68}, are up-regulated following the treatment with the cariporide and the LY294002 in the H-2452AcT cells; this appears to be a signal that occurs in response to the DNA damage and is responsible for the maintenance of the genomic-DNA integrity. Nevertheless, the DNA-repair capacity, which may provide a route for drug-resistant subpopulations to arise, was unable to override the cell-death processes that were induced by the two compounds in the H-2452AcT cells.

Oxidative stress leads to DSBs and the DNA base or deoxyribose damage causing the single-strand break (Caldecott, 2007; Karanjawala et al., 2002); moreover, excessive ROS production also triggers a mitochondrial-mediated apoptosis (Lee and Lee, 2016; Redza-Dutordoir and Averill-Bates, 2016). ROS accumulation is an early event in the cariporide-mediated anticancer effect and may trigger a rapid cell death as a consequence of intracellular acidification (De Milito et al., 2007). The combination of these results with the observations from the present study, which revealed mitochondrial damage and an apoptotic increase, indicates that the pro-oxidant role of cariporide is essential in the potentiation of the cytotoxic effects of LY294002 on H-2452AcT cells. Furthermore, it has been shown that elevated ROS levels suppress the PI3K/AKT survival pathway and subsequently induce apoptosis (Yan et al., 2015), whereas the activation of this survival pathway suppresses apoptosis via an inhibition of the apoptotic factors including the BAD (Bcl-2-associated death promoter), or via the stimulation of the transcription of the anti-apoptotic proteins including Bcl-$_{XL}$ (Fu et al., 2016). In this regard, the ROS may act as upstream molecules in the mediation of the anticancer effects of cariporide and LY294002 on the H-2452AcT cells.

In conclusion, the data of the present study suggest that the inhibition of the PI3K/AKT signaling by cariporide and LY294002 is necessary to enhance the cytotoxicity toward the acidic pHe-tolerant MM H-2452AcT cells, and that ROS-dependent mechanisms may contribute to this process. This effect seems to be mediated, at least in part, by the p53 protein that plays critical roles in the damaging of DNA, the cell cycle arrest, and apoptosis, thereby further supporting the significance of proton-pump targeting as a potential therapeutic strategy to overcome the acidic-microenvironment-associated chemotherapeutic resistance.

ACKNOWLEDGMENTS

This research was supported by Basic Science Research Program through the National Research Foundation of Korea (NRF) funded by the Ministry of Education (No. NRF-2015R1D1A3A03020269).

REFERENCES

Alfarouk, K.O. (2016). Tumor metabolism, cancer cell transporters, and microenvironmental resistance. J. Enzyme Inhib. Med. Chem. *31*, 859-866.

Astanehe, A., Arenillas, D., Wasserman, W.W., Leung, P.C., Dunn, S.E., Davies, B.R., Mills, G.B., and Auersperg, N. (2008). Mechanisms underlying p53 regulation of PIK3CA transcription in ovarian surface epithelium and in ovarian cancer. J. Cell Sci. *121*, 664-674.

Caldecott, K.W. (2007). Mammalian single-strand break repair: mechanisms and links with chromatin. DNA Repair (Amst) *6*, 443-453.

Casey, J.R., Grinstein, S., and Orlowski, J. (2010). Sensors and regulators of intracellular pH. Nat. Rev. Mol. Cell Biol. *11*, 50-61.

De Milito, A., and Fais, S. (2005). Tumor acidity, chemoresistance and proton pump inhibitors. Future Oncol. *1*, 779-786.

De Milito, A., Iessi, E., Logozzi, M., Lozupone, F., Spada, M., Marino, M.L., Federici, C., Perdicchio, M., Matarrese, P., Lugini, L., et al. (2007). Proton pump inhibitors induce apoptosis of human B-cell tumors through a caspase-independent mechanism involving reactive oxygen species. Cancer Res. *67*, 5408-5417.

Deng, L.J., Peng, Q.L., Wang, L.H., Xu, J., Liu, J.S., Li, Y.J., Zhuo, Z.J., Bai, L.L., Hu, L.P., Chen, W.M., et al. (2015). Arenobufagin

intercalates with DNA leading to G2 cell cycle arrest via ATM/ATR pathway. Oncotarget *6*, 34258-34275.

Fan, C., Zheng, W., Fu, X., Li, X., Wong, Y.S., and Chen, T. (2014). Strategy to enhance the therapeutic effect of doxorubicin in human hepatocellular carcinoma by selenocystine, a synergistic agent that regulates the ROS-mediated signaling. Oncotarget *5*, 2853-2863.

Fenouille, N., Puissant, A., Tichet, M., Zimniak, G., Abbe, P., Mallavialle, A., Rocchi, S., Ortonne, J.P., Deckert, M., Ballotti, R., et al. (2011). SPARC functions as an anti-stress factor by inactivating p53 through Akt-mediated MDM2 phosphorylation to promote melanoma cell survival. Oncogene *30*, 4887-4900.

Fu, Z., Yang, J., Wei, Y., and Li, J. (2016). Effects of piceatannol and pterostilbene against β-amyloid-induced apoptosis on the PI3K/Akt/Bad signaling pathway in PC12 cells. Food Funct. *7*, 1014-1023.

Gottlob, K., Majewski, N., Kennedy, S., Kandel, E., Robey, R.B., and Hay, N. (2011). Inhibition of early apoptotic events by Akt/PKB is dependent on the first committed step of glycolysis and mitochondrial hexokinase. Genes Dev. *15*, 1406-1418.

Guerrero-Zotano, A., Mayer, I.A., and Arteaga, C.L. (2016). PI3K/AKT/mTOR: role in breast cancer progression, drug resistance, and treatment. Cancer Metastasis Rev. *35*, 515-524.

Hu, C.F., Huang, Y.Y., Wang, Y.J., and Gao, F.G. (2016). Upregulation of ABCG2 via the PI3K-Akt pathway contributes to acidic microenvironment-induced cisplatin resistance in A549 and LTEP-a-2 lung cancer cells. Oncol. Rep. *36*, 455-461.

Igarashi, P., Freed, M.I., Ganz, M.B., and Reilly, R.F. (1992). Effects of chronic metabolic acidosis on Na(+)-H+ exchangers in LLC-PK1 renal epithelial cells. Am. J. Physiol. *263*, 83-88.

Karanjawala, Z.E., Murphy, N., Hinton, D.R., Hsieh, C.L., and Lieber, M.R. (2002). Oxygen metabolism causes chromosome breaks and is associated with the neuronal apoptosis observed in DNA double-strand break repair mutants. Curr. Biol. *12*, 397-402.

Kim, K.M., and Lee, Y.J. (2005). Amiloride augments TRAIL-induced apoptotic death by inhibiting phosphorylation of kinases and phosphatases associated with the P13K-Akt pathway. Oncogene *24*, 355-366.

Lee, Y.J., and Lee, S.H. (2016). Sulforaphane potentiates growth-inhibiting and apoptosis-promoting activities of cisplatin following oxidative stress and mitochondrial dysfunction in malignant mesothelioma cells. Mol. Cell. Toxicol. *12*, 289-299.

Lee, Y.J., Lee, D.M., and Lee, S.H. (2013). Production of Cyr61 protein is modulated by extracellular acidification and PI3K/Akt signaling in prostate carcinoma PC-3 cells. Food Chem. Toxicol. *5*, 169-176.

Lee, S., Mele, M., Vahl, P., Christiansen, P.M., Jensen, V.E., and Boedtkjer, E. (2015). Na^+, HCO_3^--cotransport is functionally upregulated during human breast carcinogenesis and required for the inverted pH gradient across the plasma membrane. Pflugers Arch. *467*, 367-377.

Ma, D., Fang, Q., Wang, P., Gao, R., Wu, W., Lu, T., Cao, L., Hu, X., and Wang, J. (2015). Induction of heme oxygenase-1 by Na+-H+ exchanger 1 protein plays a crucial role in imatinib-resistant chronic myeloid leukemia cells. J. Biol. Chem. *290*, 12558-12571.

Pabla, N., Huang, S., Mi, Q.S., Daniel, R., and Dong, Z. (2008). ATR-Chk2 signaling in p53 activation and DNA damage response during cisplatin-induced apoptosis. J. Biol. Chem. *283*, 6572-6583.

Polager, S., and Ginsberg, D. (2009). p53 and E2f: partners in life and death. Nat. Rev. Cancer *9*, 738-748.

Raghunand, N., and Gillies, R.J. (2000). pH and drug resistance in tumors. Drug Resist. Updat. *3*, 39-47.

Ramos-Nino, M.E., and Littenberg, B. (2008). A novel combination: ranpirnase and rosiglitazone induce a synergistic apoptotic effect by down-regulating Fra-1 and Survivin in cancer cells. Mol. Cancer Ther. *7*, 1871-1879.

Redza-Dutordoir, M., and Averill-Bates, D.A. (2016). Activation of apoptosis signalling pathways by reactive oxygen species. Biochim. Biophys. Acta *1863*, 2977-2992.

Rofstad, E.K., Mathiesen, B., Kindem, K., and Galappathi, K. (2006). Acidic extracellular pH promotes experimental metastasis of human melanoma cells in athymic nude mice. Cancer Res. *66*, 6699-6707.

Rohwer, N., and Cramer, T. (2011). Hypoxia-mediated drug resistance: novel insights on the functional interaction of HIFs and cell death pathways. Drug Resist. Updat. *14*, 191-201.

Schmitt, C.A., and Lowe, S.W. (2001). Bcl-2 mediates chemoresistance in matched pairs of primary E(mu)-myc lymphomas in vivo. Blood Cells Mol. Dis. *27*, 206-216.

Singh, M., Bhui, K., Singh, R., and Shukla, Y. (2013). Tea polyphenols enhance cisplatin chemosensitivity in cervical cancer cells via induction of apoptosis. Life Sci. *93*, 7-16.

Skammeritz, E., Omland, L.H., Johansen, J.P., and Omland, O. (2011). Asbestos exposure and survival in malignant mesothelioma: a description of 122 consecutive cases at an occupational clinic. Int. J. Occup. Environ. Med. *2*, 224-236.

Souza, R.F., Shewmake, K., Terada, L.S., and Spechler, S.J. (2002). Acid exposure activates the mitogen-activated protein kinase pathways in Barrett's esophagus. Gastroenterology *122*, 299-307.

Tomita, M. (2010). Involvement of DNA-PK and ATM in radiation- and heat-induced DNA damage recognition and apoptotic cell death. J. Radiat. Res. *51*, 493-501.

Warburg, O. (1956). On the origin of cancer cells. Science *123*, 309-314.

Weller, M. (1998). Predicting response to cancer chemotherapy: the role of p53. Cell Tissue Res. *292*, 435-445.

Wilson, S.M., Barbone, D., Yang, T.M., Jablons, D.M., Bueno, R., Sugarbaker, D.J., Yoshida, G.J. (2015). Metabolic reprogramming: the emerging concept and associated therapeutic strategies. J. Exp. Clin. Cancer Res. *34*, 111.

Wong, P., Kleemann, H.W., and Tannock, I.F. (2002). Cytostatic potential of novel agents that inhibit the regulation of intracellular pH. Br. J. Cancer *87*, 238-245.

Wu, K.L., Khan, S., Lakhe-Reddy, S., Jarad, G., Mukherjee, A., Obejero-Paz, C.A., Konieczkowski, M., Sedor, J.R., and Schelling, J.R. (2004). The NHE1 Na^+/H^+ exchanger recruits ezrin/radixin/moesin proteins to regulate Akt-dependent cell survival. J. Biol. Chem. *279*, 26280-26286.

Yan, C.M., Chai, E.Q., Cai, H.Y., Miao, G.Y., and Ma, W. (2015). Oleuropein induces apoptosis via activation of caspases and suppression of phosphatidylinositol 3-kinase/protein kinase B pathway in HepG2 human hepatoma cell line. Mol. Med. Rep. *11*, 4617-4624.

Yoshida, G.J. (2015). Metabolic reprogramming: the emerging concept and associated therapeutic strategies. J. Exp. Clin. Cancer Res. *34*, 111.

Zheng, Y.T., Yang, H.Y., Li, T., Zhao, B., Shao, T.F., Xiang, X.Q., and Cai, W.M. (2015). Amiloride sensitizes human pancreatic cancer cells to erlotinib in vitro through inhibition of the PI3K/AKT signaling pathway. Acta Pharmacol. Sin. *36*, 614-626.